INTERSECTII
http://www.intersections.ro
INTERSECTIONS

Performance Evaluation of Dual-eccentrically Braced Frames

Gabriel-Alexandru Sabau, Aurel Stratan
Department of Steel Structures and Structural Mechanics, Politehnica University Timisoara, 200224, Romania

Summary

The later force resistance in dual-eccentrically braced frames is provided by two structural system: eccentrically braced frames (the primary sub-system) and moment-resisting frames (the secondary sub-system). Eccentrically braced frames dissipates most of the seismic energy through plastic deformations in links, while moment-resisting frames represent a back-up system, increases the redundancy of the overall system. This paper presents the modelling approach of steel dual-eccentrically braced frames using the OpenSees software framework. Ten different structural configurations were used to evaluate their performance given two levels of seismic hazard. The analyses of the frames is part of the ongoing European pre-QUALified steel JOINTS project, concerned with the pre-qualification of all-steel Beam-to-Column joints in steel structures. The designed frames were evaluated in terms of seismic performance by means of non-linear static (pushover) analyses, with a modal and uniform distribution of forces, time history and incremental dynamic analyses. The eccentrically braced frame contains short links, for which the shear force - shear deformation (V-γ) curve was calibrated based on experimental results. The physical theory models were used for columns and braces in the numerical model. The model was built in a 3D environment and extra nodes were added at each column and brace midpoint to account for initial imperfections. The midpoints were without restraints so that buckling could occur about the weak axis.

KEYWORDS: steel dual-eccentrically braced frames, short links, OpenSees, IDA analysis, performance evaluation, FEM modelling, physical theory models

INTRODUCTION

An inverted “V” (Chevron) configuration was chosen for the dual eccentrically-braced frames. The braces are located at the central bay of each frame and are assumed to have out-of-plane pinned ends and rigid in-plane connections. The seismic links are horizontal, located at the beam where the braces converge and have a uniform length of 0.7m, which leads to a “short” link design, for the specific range of selected member sizes. The section of the link is the same as the section of the adjacent beam (using full-depth web stiffeners to ensure ductile cyclic behaviour, per EN 1998-1 [5], Section 6.8.2). The exterior bays are modelled as

ISSN 1582-3024

INTERSECTII
INTERSECTIONS
http://www.intersections.ro

moment resisting frames. Square hollow sections (i.e. SHHF or SHS) are selected for the braces and HEA sections are selected for the seismic links/beams. The beam-column joints are considered to be full strength and fully rigid connections. The structures analysed are presented in Table 1 .

Table 1 Designed dual-eccentrically braced frames

Frame Name	Structural Configuration
DEBF-6-3-6-MH	D-EBF, 6-storey, 3-bay, 6m span, PGA=0.25g
DEBF-6-3-6-HH	D-EBF, 6-storey, 3-bay, 6m span, PGA=0.35g
DEBF-6-3-8-MH	D-EBF, 6-storey, 3-bay, 8m span, PGA=0.25g
DEBF-6-3-8-HH	D-EBF, 6-storey, 3-bay, 8m span, PGA=0.35g
DEBF-6-5-6-HH	D-EBF, 6-storey, 5-bay, 6m span, PGA=0.35g
DEBF-12-3-6-MH	D-EBF, 12-storey, 3-bay, 6m span, PGA=0.25g
DEBF-12-3-6-HH	D-EBF, 12-storey, 3-bay, 6m span, PGA=0.35g
DEBF-12-3-8-MH	D-EBF, 12-storey, 3-bay, 8m span, PGA=0.25g
DEBF-12-3-8-HH	D-EBF, 12-storey, 3-bay, 8m span, PGA=0.35g
DEBF-12-5-6-HH	D-EBF, 12-storey, 5-bay, 6m span, PGA=0.35g

BASIC MODELLING ASSUMPTIONS FOR DEBFS

The OpenSees model of the structure was defined in a 3D environment. Out of plane degrees of freedom were blocked for the nodes connecting beams, columns and braces. The 3D model allows for imperfections to be introduced in the columns and braces. The imperfections were added by inserting off-plane mid-points with an offset of L/1000 [9]. These nodes have 6 degrees of freedom allowing the elements to gain out-of-plane deformations. Except for the braces which have pinned out-of-plane connections and rigid in-plane connections, all the other elements have rigid connections. The columns' web panel was considered to be fully rigid. To model the rigid web panel nodes were added at the beams and columns flange positions as seen in Figure 4. These nodes were connected to the central node through rigid elements. The second order effects were taken into account by modelling a leaning column with the additional loads of the rest of the

ISSN 1582-3024

INTERSECTII
http://www.intersections.ro

structure. The masses were assigned to the leaning-column nodes. A typical structural scheme showing element connectivity is shown in Figure 1.

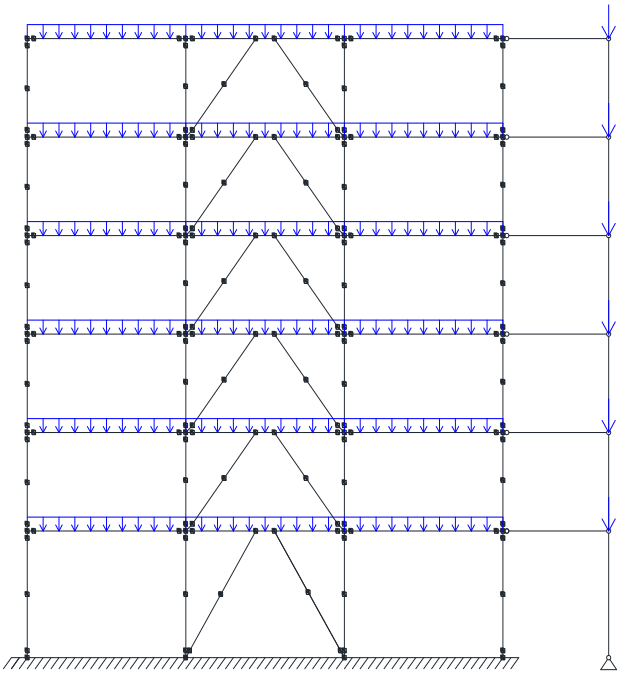

Figure 1. Structural model with nodes position

Beams, columns and braces were modelled as fiber sections with 20 fibres along the flange and web length, and 2 fibers along the flange and web thicknesses respectively. The sections were attributed to force controlled elements with distributed plasticity (forceBeamColumn). Three integration points were attributed to each half length of the columns and braces, five integration points for the beams and three for the links.

The link was modelled by aggregating the shear force-deformation response with a forceBeamColumn element accounting for flexural deformations. The shear response was modelled with a Steel4 [1] hysteretic relationship material with the yielding strength equal to the yielding force of the link element in shear calculated with Equation (1) and the initial stiffness of the link accounting only for shear Equation (1) (disregarding the contribution of the flexural stiffness). The stiffness was inserted as the ratio between shear force and shear deformation (V-γ). The modelling parameters for links values are shown in Table 2.

ISSN 1582-3024

$$V_y = \frac{A_{vz} \cdot f_y}{\sqrt{3} \cdot \gamma_{MI}} \quad (1)$$

$$K_s = \frac{G \cdot A_{vz}}{e} \quad (2)$$

$$\gamma_y = \frac{V_y}{K_s \cdot e} \quad (3)$$

Table 2. Links shear modelling parameters

Link Section	Vy [kN]	K_s [kN/rad]	γ_y [rad]	γ_u [rad]
HE450A	1218.6	370737		
HE400A	1030.9	313632		
HE360A	922.5	280665		
HE340A	751.2	228541		
HE320A	668.5	203391		
HE300A	592.4	180387	0.00329	0.15
HE280A	519.7	158112		
HE260A	449.3	136687		
HE240A	411.3	125145		
HE220A	350.4	106596		
HE200A	294.2	89505		
HE180A	242.8	73872		

*V_y = force at yield; θy = link rotation at yield; θu = link rotation at failure;

The shear behaviour of the link was calibrated based on the experimental results from Okazaki and Engelhardt 2006 [11] on short links. The model used for the calibration consisted in a 2D beam element with all the degrees of freedom blocked at one end and rotation blocked at the other end. Fiber sections were used to define the cross-section of the element, just as in the large structural model. The material parameters determined for the link response are presented in

Table 3.

Table 3. Steel4 material parameters

Parameter	Parameter description	Value
b_k	Kinematic hardening ratio	0.018
R_0	Controls the exponential transition from elastic to plastic asymptote	15
r_1		0.82
r_2		0.2
b_i	Isotropic hardening ratio	0.0032

ISSN 1582-3024

b_l	Isotropic saturated hardening ratio	0.0014
rho_i	Position of intersection point between initial and saturated asymptote	0.24
R_i	Controls the exponential transition from initial to saturated isotropic hardening	50
l_yp	Length of the yielding plateau	0
f_u	Ultimate strength	$1.5 \cdot V_y$
R_u	Controls the transition from kinematic hardening to perfectly plastic asymptote	1.8

*V_y = force at yield as described in Table 2 taken for each link according to its cross-section properties

The calibrated link used from Okazaki and Engelhardt 2006 [11] was a W10x33 with the length of 584 mm subjected to a revised loading protocol according to 2005 AISC Seismic Provisions [3]. The static scheme used for the analyses can be seen in Figure 2.

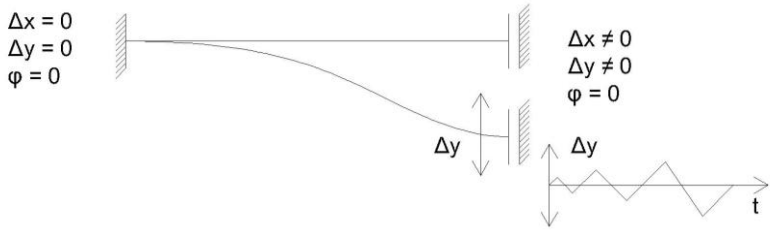

Figure 2. Link calibration static scheme

The comparison between the numerical and experimental results are displayed in Figure 3 in terms of shear force – element rotation.

ISSN 1582-3024

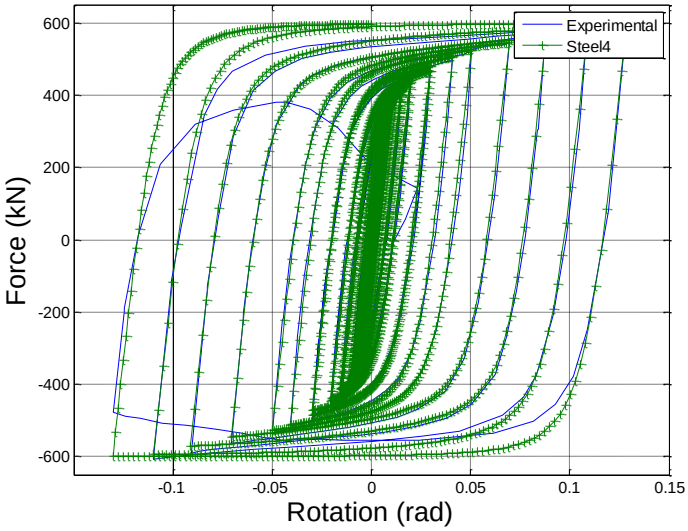

Figure 3. Numerical validation of shear link element

The leaning column was modelled using elastic elements (elasticBeamColumn) with the cross-section properties of the 4 central columns for the 3-bay model and 6 columns for the 5-bay model. The transformation methods assigned to each type of element can be seen in Table 4.

Table 4 Element modelling parameters

Structural element	Finite element type	Section	Transformation
Beam	forceBeamColumn	Fibre section	Linear
Brace	forceBeamColumn	Fibre section	Corotational
Column	forceBeamColumn	Fibre section	Corotational
Seismic link	forceBeamColumn	Fibre section	Linear
Leaning column	elasticBeamColumn	Elastic section	P-Delta
Rigid link element	elasticBeamColumn	Elastic section	Linear

The elements go from node to node with a rigid offset to account for the height of the beams and columns as seen in Figure 4. This is to model the panel zone as a fully rigid part of the structure. The nodes are considered to be full strength and fully rigid.

ISSN 1582-3024

INTERSECTII
http://www.intersections.ro

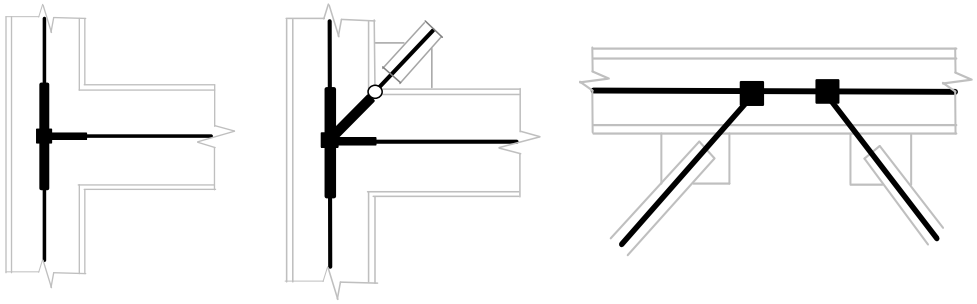

a) b) c)

Figure 4. Model of connection types: beam-column joint (a), beam-brace column (b), brace link (c)

The material for all frame elements is S355 steel with an over-strength factor γov= 1.25. The chosen member sections are standard metric sections. The materials used for the fibre sections was Steel02 [12] (Giuffré-Menegotto-Pinto Model with Isotropic Strain Hardening) with the parameters values specified in Table 5.

Table 5. Steel02 modelling parameters

f_y, [N/mm^2]	E, [N/mm^2]	b	R0	cR1	cR2
443.5	210000	0.02	18	0.925	0.15

*f_y = steel yield stress; E = steel modulus of elasticity; b = strain hardening ratio; *R0*, *cR1*, *cR2* = control the transition from elastic to plastic branches

ANALYSIS RESULTS

Modal analysis

The results of the eigenvalue analysis in terms of 1st and 2nd modal periods of the moment frames are summarized in

Table 6. The range of the fundamental natural periods of vibration is from 0.93 to 1.14s for the 6-storey typologies and from 1.60s to 1.86s for the 12-storey typologies.

Table 6. Natural periods of vibration of DEBFs

Frame	T_1 (s)	T_2 (s)	Frame Typology	T_1 (s)	T_2 (s)
DEBF-6-3-6-MH	1.00	0.35	DEBF-12-3-6-MH	1.78	0.60

ISSN 1582-3024

INTERSECTII
http://www.intersections.ro

DEBF-6-3-6-HH	0.93	0.33	DEBF-12-3-6-HH	1.60	0.54
DEBF-6-3-8-MH	1.14	0.41	DEBF-12-3-8-MH	1.86	0.62
DEBF-6-3-8-HH	1.00	0.36	DEBF-12-3-8-HH	1.67	0.56
DEBF-6-5-6-HH	0.97	0.35	DEBF-12-5-6-HH	1.59	0.55

Pushover analysis

The frame typologies presented in Table 1 were subjected to pushover analyses, using both a uniform lateral load distribution and a modal lateral load distribution [10]. The control parameter is the top floor horizontal displacement. The computed pushover curves are presented in Figure 5 for the 6-storey frames and in Figure 6 for the 12-storey frames. The pushover curves for the structures with 6 m bays and 6 storeys show an increase of shear force over the plastic plateau mainly due to the overstrength [8] of the seismic links. Structures with larger spans and more storeys show a local failure mechanism due to the buckling of the compressed braces from the lower storeys. After the buckling occurs, an increased sensitivity to second order effects can be noticed in the structure. This happens at very large roof displacements (approx. 6% drift). The post-yielding plateau of the pushover curve is decreasing, response generated by a storey failure mechanism in addition to the second order effect, leading to a fragile failure mechanism. The 5 bays frames show ductility and an increase in the post-yielding stiffness, regardless of the number of storeys. On the other hand, it can be observed that the uniform load pattern leads to larger base shear force.

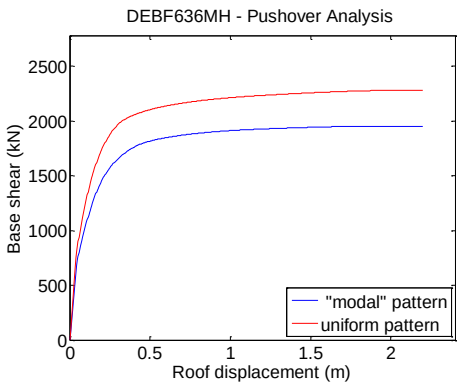

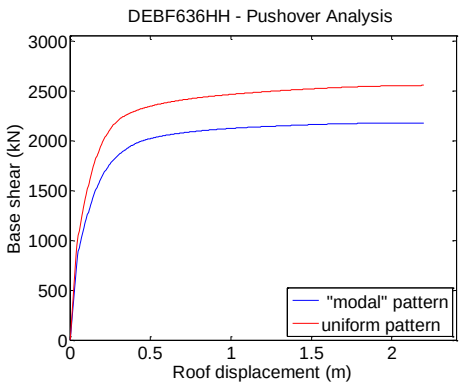

ISSN 1582-3024

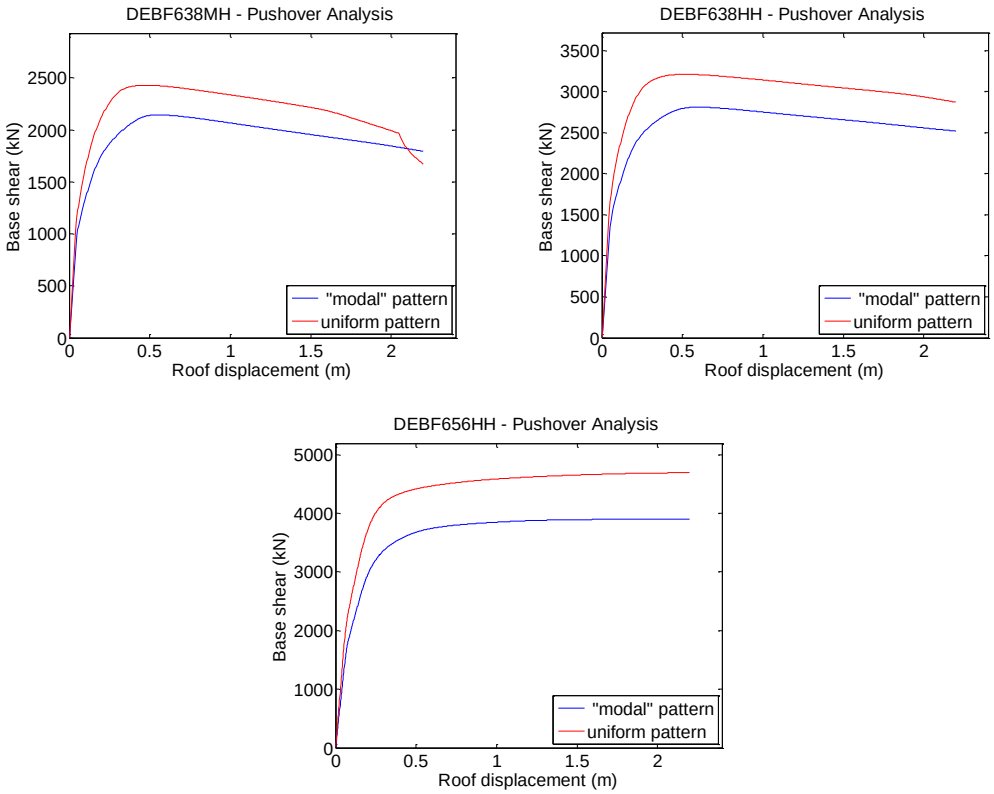

Figure 5. Pushover curves for 6-storey DEBFs

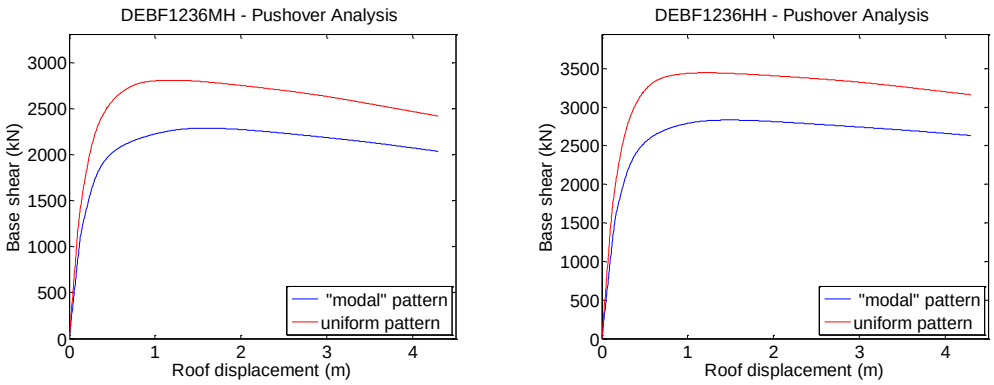

INTERSECTII
http://www.intersections.ro

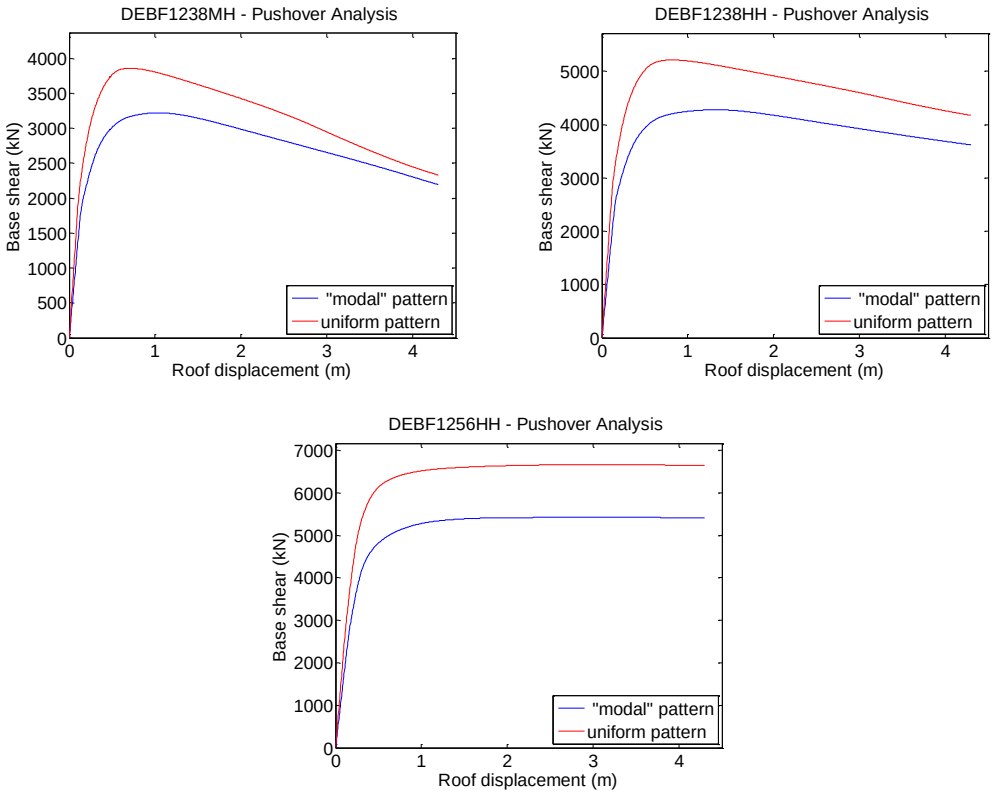

Figure 6. Pushover curves for 12-storey DEBFs

Non-linear dynamic analysis

The set of dual eccentrically braced frames was used for performing dynamic analyses, using as ground acceleration input two ground motion suites, for high seismic hazard (HH) and medium seismic hazard (MH) [1]. Rayleigh damping was used for a ratio ξ_i = 2% at the first and third natural frequencies of vibration. To monitor the residual displacements and deformations, additional 10 seconds were added to each accelerogram with 0 acceleration input. For the last 10 seconds the damping ratio was increased to ξ_r = 20%. Three performance objectives (limit states) were considered, according to EN 1998-3 (CEN 2005b) [5]: damage limitation (DL), significant damage (SD), near collapse (NC). The corresponding seismic intensity levels were, respectively 50%, 100% and 175%, of the design one. The basic parameters monitored were the maximum and residual inter-storey drift ratios, link and beam rotations.

ISSN 1582-3024

INTERSECTII
http://www.intersections.ro

Inter-storey drift ratios

As seen in Figure 7 for the 6-storey frames the peak inter-storey drifts occur at the 2nd and 3rd storey and range from 0.014 rad for the MH cases up to 0.019 rad for the HH cases. The residual inter-storey drifts keep the same profile as the maximum values with the peaks at the 2nd and 3rd storey. The values range from 0.0011 rad for the MH cases to 0.0074 rad for the HH cases .In the case of the 12-storey frames, peak inter-storey drifts occur at the 3rd and 4th storeys of the frames and vary from 0.019 rad to 0.029 rad for the HH cases. The peak inter-storey drift for the MH frames occur at mid-height between the 5th and 6th storey. The values range between 0.0093 rad and 0.0095 rad, showing a reduced influence of the span's length. Same as for the 6-storey frame the residual inter-storey drift has the peaks were the maximum value for drift occurred. It can be seen that the values for residual inter-storey drift ranges from 0.0012 rad for MH frames to up to 0.0075 rad for HH frames.

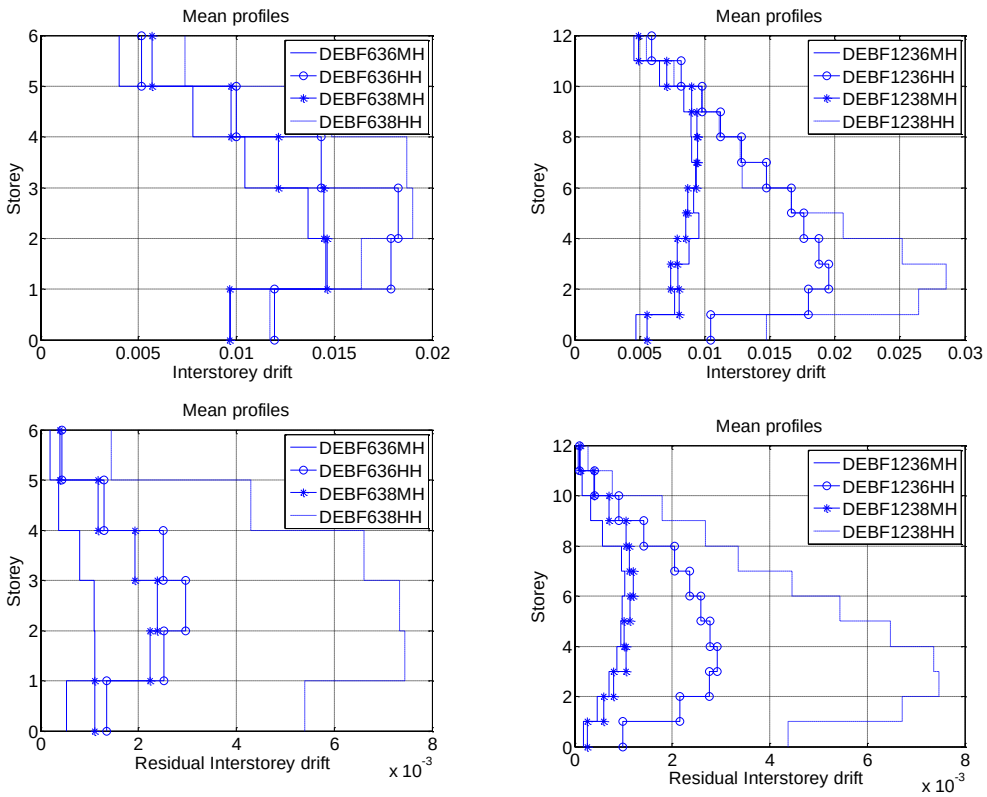

Figure 7. Mean profiles of max. and residual inter-storey drift ratios for the near collapse performance level

ISSN 1582-3024

Link deformations

The acceptance criteria for link deformations in terms of plastic rotation for the 3 limit states considered are taken from ASCE/SEI 41-13 [42], were the corresponding limit states are immediate occupancy (IO), life safety (LS) and collapse prevention (CP). The structures were verified that the elements requirements are within the accepted limits as seen in Table 7. For the DL limit state, the links rotations exceed the acceptance criteria in all the frames considered as opposed to the SD limit state. The link rotations for the SD limit state are much lower than the accepted ones (the lowest being 5 times less in the DEBF-12-3-6-MH frame). At the CP limit state the links that exceed the acceptance criteria are the ones from the 8 m spans frames designed for high seismic hazard. Comparing the link rotation from the 6 m span and the 8 m span frames, it can be seen that the link has a higher contribution when wider spans are implied.

Table 7. Performance evaluation of link elements

	Mean profile of link max rotation			Acceptance criteria		
Frame	DL (IO)	SD (LS)	NC (CP)	IO	LS	CP
DEBF-6-3-6-MH	0.0156*	0.0375	0.073	0.005	0.14	0.16
DEBF-6-3-6-HH	0.0231*	0.0598	0.134			
DEBF-6-3-8-MH	0.0193*	0.0514	0.102			
DEBF-6-3-8-HH	0.0345*	0.0763	0.186*			
DEBF-12-3-6-MH	0.0127*	0.0294	0.059			
DEBF-12-3-6-HH	0.0160*	0.0464	0.072			
DEBF-12-3-8-MH	0.0158*	0.0356	0.098			
DEBF-12-3-8-HH	0.0206*	0.0580	0.166*			

*the deformation requirement exceeds the acceptance criteria

Beam deformations

As described in paragraph 0 the same checks were made for the beam rotations. As seen in Table 8 the mean profile of beam rotations does not exceed the acceptance for none of the limit states considered. The values are much lower than the accepted ones by almost 5 times, even at DL limit state. This shows that the MRF beams do not suffer large deformations even at high seismic intensities. The MRF could serve this way as a backup for the failure of the EBF.

Table 8. Performance evaluation of beams

	Mean profile of beam max rotation			Acceptance criteria		
Frame	DL (IO)	SD (LS)	NC (CP)	IO	LS	CP
DEBF-6-3-6-MH	0.0047	0.0080	0.0151	0.0247	0.117	0.143
DEBF-6-3-6-HH	0.0063	0.0114	0.0242	0.0247	0.117	0.143
DEBF-6-3-8-MH	0.0054	0.0094	0.0171	0.0342	0.162	0.198
DEBF-6-3-8-HH	0.0081	0.0127	0.0266	0.0342	0.162	0.198
DEBF-12-3-6-MH	0.0058	0.0083	0.0129	0.0228	0.108	0.132
DEBF-12-3-6-HH	0.0073	0.0116	0.0224	0.0228	0.108	0.132

ISSN 1582-3024

DEBF-12-3-8-MH	0.0060	0.0091	0.0126	0.0304	0.144	0.176
DEBF-12-3-8-HH	0.0080	0.0123	0.0328	0.0304	0.144	0.176

Incremental dynamic analysis

For performing incremental dynamic analyses (IDA) [7], the same ground acceleration input as for the time-history analyses was used. The parameters were kept unmodified. The ground motions were scaled by factors ranging from 0.25% to 400% at a constant step of 0.25%. The basic parameters monitored are the maximum inter-storey drift ratios (directly related to the rotation demands on connections) and the absolute storey accelerations (related to non-structural damage). Representative IDA curve sets in terms of maximum inter-storey drift ratio vs. ground motion intensity are presented in the plots of Figure 8. From the inter-storey drift IDA curve sets most of the frames considered, exhibit a hardening behaviour, with increasing ground motion intensity. However for the HH frames at higher seismic intensities, above 200% a soft storey mechanism begins to show. The IDA curves show a hardening mean response for all the considered frames. In the case of the 00293T accelerogram for HH frames, a softening behaviour can be observed, together with an intermediate collapse area followed by a structural resurrection. At different seismic intensities the global response of the structure changes, due to different failure mechanisms.

At the Damage Limitation (DL) performance level (corresponding to ground motion intensity 100%), the inter-storey drifts range approximately between 0.0075 rad and 0.012 rad, on average, which is much lower than the generally accepted ultimate drift levels for connections (0.035-0.040 rad). The latter levels of deformation are attained at intensities close to 350% (corresponding to two times the NC performance level) for the MH frames and around 175% for the HH frames.

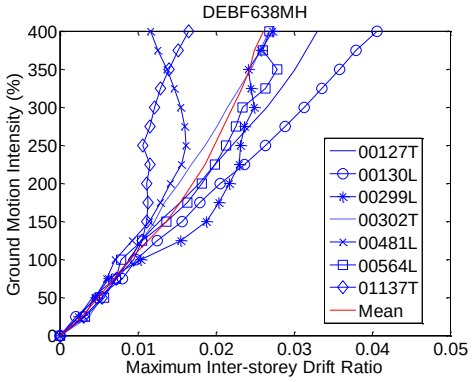

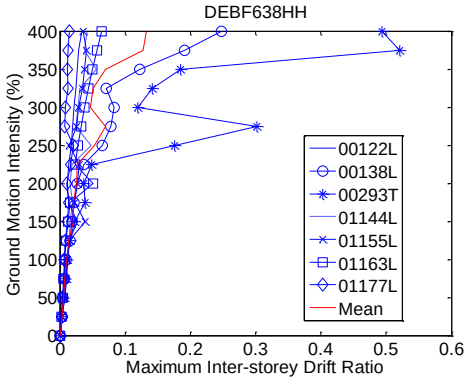

INTERSECTII
http://www.intersections.ro

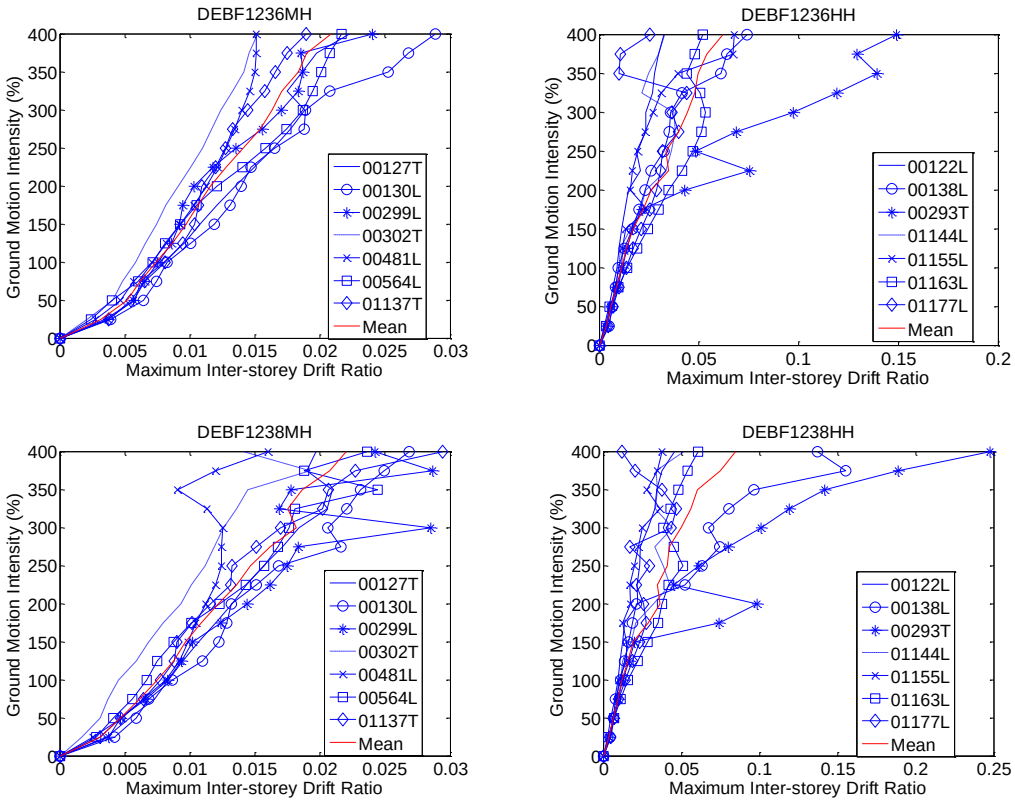

Figure 8. IDA curves maximum inter-storey drift ratio

IDA curve sets for maximum floor accelerations (absolute) vs. ground motion intensity for the 6-storey frame typology MRF636 (MH and HH) are presented in Figure 9. The peak recorded absolute accelerations are systematically recorded at the top floor of the frames. The dynamic amplification with respect to the peak ground acceleration is of the order of 400%.

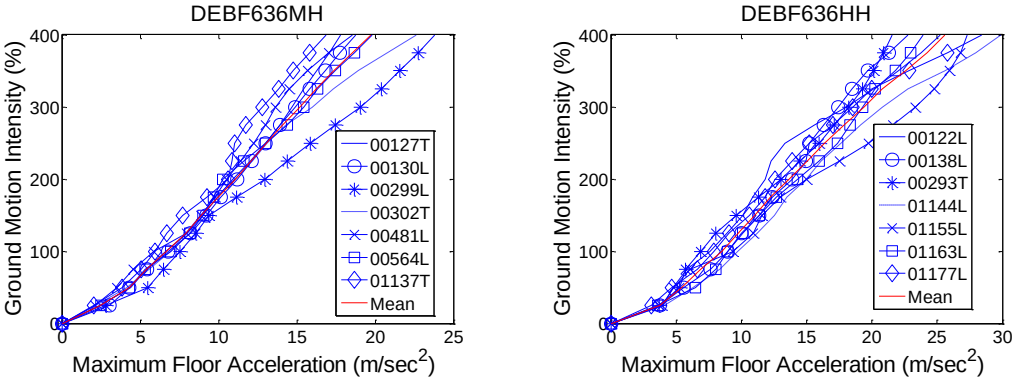

ISSN 1582-3024

INTERSECTII
http://www.intersections.ro
INTERSECTIONS

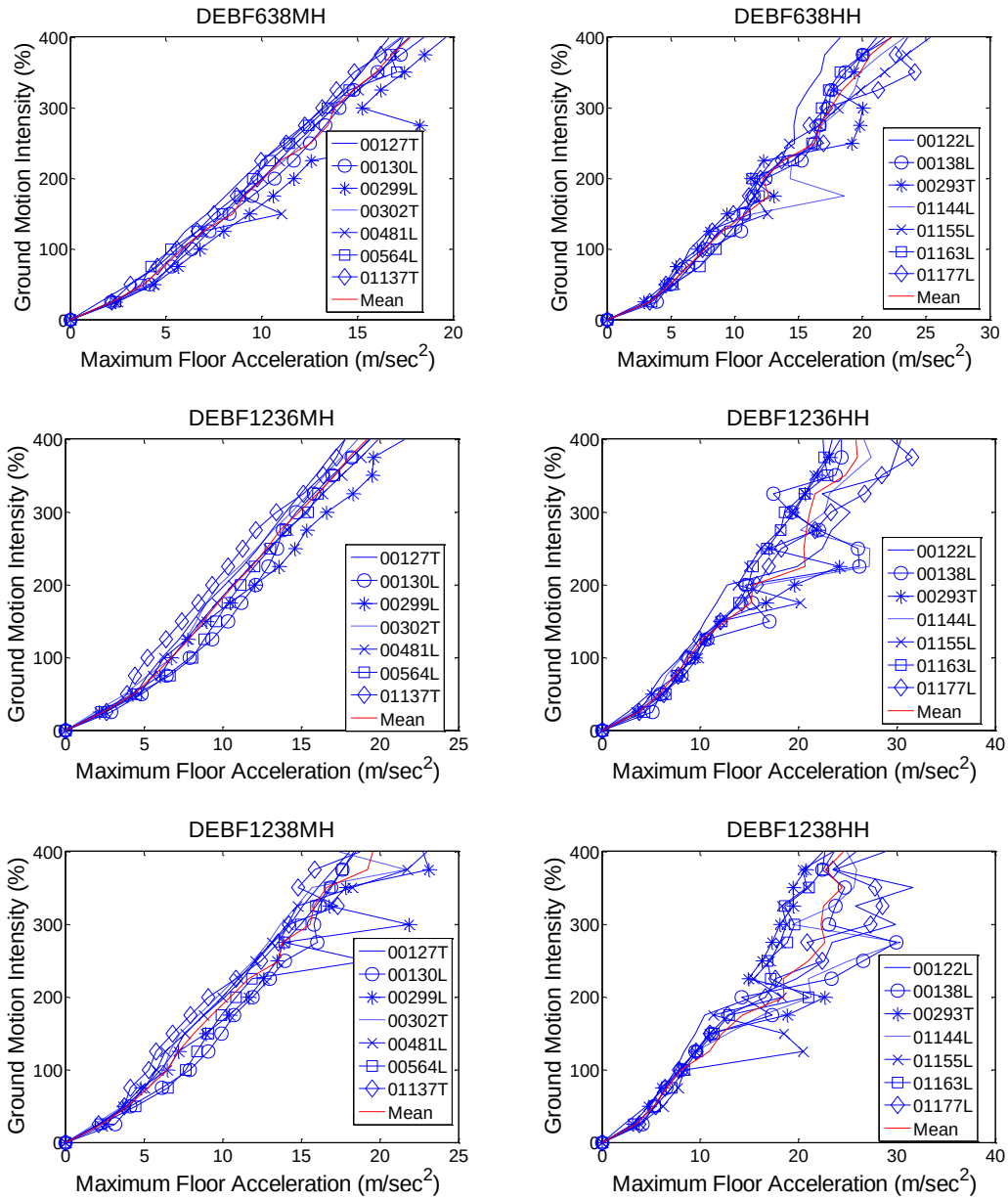

Figure 9. IDA curves maximum floor acceleration

ISSN 1582-3024

INTERSECTII
INTERSECTIONS
http://www.intersections.ro

CONCLUSIONS

The 3D modelling approach allows the designer to check the structure's response including the buckling of compressed elements. This type of modelling gives a more realistic feedback of the structural behaviour. At the same the analysis and the results processing requires more resources and time.

As presented in the previous chapters the pushover results give valuable insights of the general behaviour of the considered frames. Different failure modes can be observed, varying from global failure of the frame through hardening behaviour to local failure of elements through a softening plateau. It can be seen that the P-delta effects have a large impact on the response of the structure, especially when imperfection are included in the model.

The time history analysis shows that for medium seismic hazard, the length of the bays has a negligible influence on the response of the structures (in terms of inter-storey drift), even at the near collapse limit state. For structures subjected to high seismic hazard, the span has a big influence on the response of the structure, leading to an absolute inter-storey drift increase of almost 50% from a 6 m span to an 8 meter span. The residual inter-storey drift is also increased by 2.5 times.

At element level, the two monitored deformations show that for the first limit state (DL) all the links exceed the acceptance criteria, whereas the beams have minor deformations. For the SD limit state neither of the two exceed the accepted values. At the CP limit state only links from 2 of the HH frames, with 8 m span length exceed the accepted rotation.

The performance of the structures can be further analysed in terms of elements behaviour to identify if the non-dissipative elements requirements are within the acceptance criteria; their design strength is not exceeded.

Acknowledgements

The research leading to these results has received funding from the European Community's Research Fund for Coal and Steel (RFCS) under grant agreement no RFSR-CT-2013-00021 "European pre-qualified steel joints (EQUALJOINTS)". This support is gratefully acknowledged.

References

1. A. Tsitos, A. Elghazouli, *European pre-QUALified steel JOINTS: Provisional design of protype building and selection of strong motions records, Rev.02*. Imperial College London. July 2014
2. A. Zsarnóczay, L.G. Vigh, *Experimental and Numerical Investigation of Buckling Restrained Braced Frames for Eurocode Conform Design Procedure Development*, Budapest University of Technology and Economic, Budapest, 2013.

ISSN 1582-3024

3. American Institute of Steel Construction, Inc. (AISC) (2010). *Seismic provisions for structural steel buildings*. Standard ANSI/AISC 341-10. Chicago (IL, USA).
4. ASCE/SEI 41-13: American Society of Civil Engineers: seismic evaluation and retrofit of existing buildings. ASCE standard. ISBN 978-0-7844-1285-5
5. CEN (2004). Eurocode 8: Design of structures for earthquake resistance – Part 1: General rules, seismic actions and rules for buildings. European Standard EN 1998-1:2004, Brussels.Eurocode 8
6. CEN (2004a). Eurocode 3: Design of steel structures – Part 1-1: General rules and rules for buildings. European Standard EN 1993-1-1:2004, Brussels.
7. D. Vamvatsikos and C. Allin Cornell. *Incremental dynamic analysis* Department of Civil and Environmental Engineering; Stanford University; CA 94305-4020; U.S.A.
8. G. Della Corte, M. D'Aniello, F.M. Mazzolani, (2008). *Overstrength of Shear Links in Eccentric Braces*. 15th World Conference on Earthquake Engineering, Lisbon.
9. EN 10034: 1993. "Structural steel I and H sections. Tolerances on shape and dimensions".
10. FEMA 356 (2000). "Prestandard and commentary for the seismic rehabilitation of buildings". Federal Emergency Management Agency;
11. Okazaki T., Engelhardt M. D. (2007). *Cyclic loading behaviour of EBF links constructed of ASTM A992 steel*. Journal of constructional Steel Research, 63, 751-765.
12. OpenSees (2015). *Open System for Earthquake Engineering Simulation*, Pacific Earthquake Engineering Research Center, University of California at Berkeley, California USA (opensees.berkeley.edu as of March 10th 2015).

Appendix

λ	Hazard level amplification factor
f_y	Steel yield stress
A_{vz}	Effective shear area of steel section
G	Shear elastic modulus
γ_{MI}	Material safety factor
e	Link length
E	Steel modulus of elasticity
b	Strain hardening ratio
γ_{ov}	Steel overstrength coefficient
V_y	Shear yield force
V_u	Shear ultimate force
K_s	Link shear elastic stiffness of element
γ_y	Link yield shear deformation
γ_u	Link ultimate shear deformation

ISSN 1582-3024